Scientific Report

For the project "**Novel conjugated polymer structures for high efficiency all-organic solar cells**"
Code: PN-II-ID-PCE-2011-3-0274

Phase 2015

Objective 1: *New acceptor compounds, as substitutes of fullerene.*
***Task** 1.1. Studies of new acceptors: graphene oxide, graphene, perylenediimide.*
***Task** 1.2. Structural characterization of acceptors.*

Solar cells build with organic conjugated polymers are based on the heterojunction configuration (BHJ, bulk heterojunction) [1-4]. Heterojunction interface provides greater separation surface between donor and acceptor and therefore an increased efficiency in dissociation of exciton formed by absorbing sunlight into charge carriers. In the solar cells based on inorganic compounds, the light absorption leads to free charge carriers which then are moved to the electrodes due to the internal electric field. In organic compounds light absorption leads to the formation of an excited state (exciton), which is a loosely bounded electron / hole pair, that can free move into the mass of material. Exciton dissociation in free charge carriers takes place at the surface of separation between donor and acceptor before being collected by electrodes. For a high efficiency in exciton dissociation the two partners must be mixed at the nanometer level, forming uniform islands of the order of 10-20 nm, so how is the effective exciton diffusion distance. The photoactive layer sandwiched between two electrodes is a bicontinuos interpenetrating network between donor and acceptor at the nanometer level, ensuring a great separation interface. Basically, both donor and acceptor are dissolved in an organic solvent to obtain a homogeneous solution which is then deposited in the form of film on a transparent electrode (ITO) by known techniques (i.e., spin-coating).
As is known, in the BHJ-type solar cells four steps are important: (i) absorption and generation of excitons, (ii) difusion and exciton dissociation at the donor / acceptor interface, (iii) carriers transport to the electrodes, and (iv) collection of carriers by electrodes. An ideal solar cell should meet the following requirements: (i) a high local order local to ensure a strong absorption of photons in the whole solar spectrum, transport of excitons and charge carriers, (ii) the phase separation between the donor and acceptor materials, which should form a continuous entangled network of the donor and acceptor with domain sizes similar to the exciton diffusion length of about 10-20 nm, and (iii) formation by segregation of specific channels transport for electrons and holes. A schematic solar cell made using a new polymer [poly (N-2'-ethylhexyl) 2,7-carbazolyl -vinylene] / fullerene (its synthesis was reported in the previous years) is presented in Figure 1.

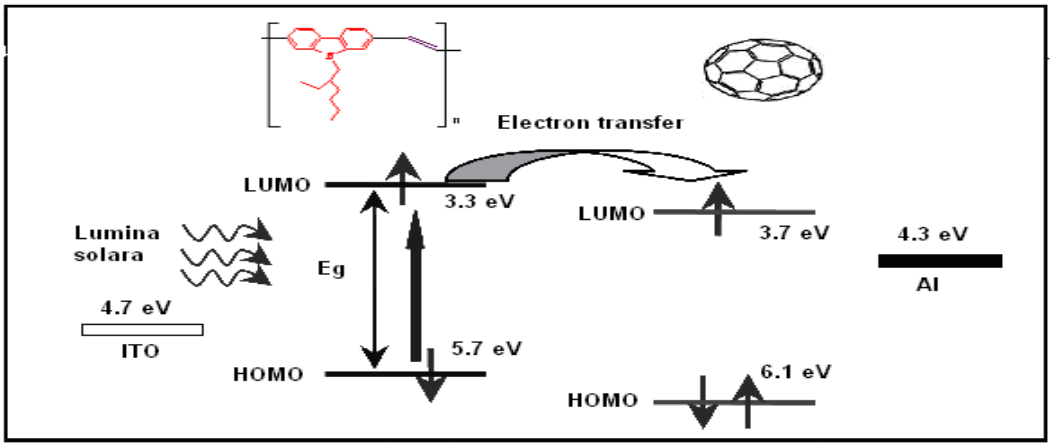

Figure 1: Photovoltaic effect in a solar cell based on [poly (N-2'-ethylhexyl) 2,7-carbazolyl vinylene] si fullerene.

Unfortunately, the forbidden band (~ 2.4 V) of poly (N-2'-ethylhexyl) 2,7-carbazolyl vinylene is not enough small to take on an extended absorption of the solar spectrum. This deficiency can be overcome by using a donor/acceptor copolymer. To ensure an efficient exciton dissociation, the donor LUMO energy level (-3.3 eV) must be higher than that of the acceptor (-3.7 eV) providing electron transfer from D to A. Most studies so far have used conjugated polymers of p-type while fullerene and its derivatives (C60, C71) as electron acceptor, but which are expensive materials. However, fullerene acceptors have disadvantages, such as relatively weak absorption ability in the visible region due to their symmetrical structures; the need for high purity, making their synthesis very expensive; thermally unstable morphology of polymer/fullerene blend films due to the rapid diffusion of fullerene molecules; and restricted chemical and energetic tunability, which limits the design of complementary polymer donors for maximum solar cell performance, in particular for enhancing the Voc and short-circuit current (Jsc) simultaneously.

Other allotropes of carbon have been tried in place of fullerenes, i.e., carbon nanotubes (single or multi, SWNT, MWNT). However, few adverse factors as insolubility, impurities, bundles of nanotubes structure did not permit obtaining of good performance for such solar cells.

Graphene (Figure 2, A), a component of graphite, is a monolayer of carbon atoms in a sp^2 hybridized state which attracted major interest in recent years, especially since the first experimental evidence of the electronic properties of graphene in 2004 [5]. Graphene is a semiconductor without a band gap (with Eg ~ 0) with unique electronic properties, a very high electron mobility (100,000 cm^2 / Vs), a very good thermal conductivity (5000 $Wm^{-1}. K^{-1}$) superior mechanical properties with an Yang modulus of 1 TPA and can be used in very different applications [6-8].

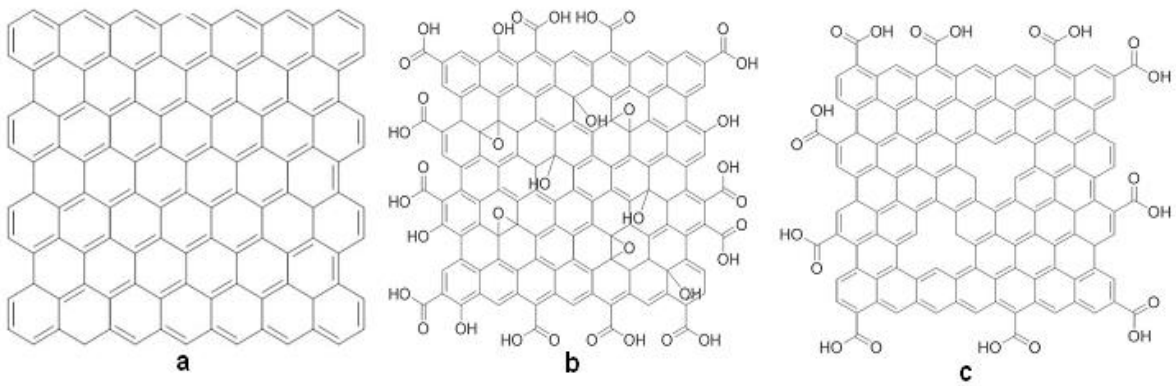

Figura 2: The structure of graphene (a), grapheme oxide, GO (b) and graphene obtained after GO reduction (c)

Various methods have been developed for obtaining of graphene; a) physical methods and b) chemical methods. In graphite, graphene adjacent layers are held together by weak van der Waals forces [9], therefore graphene can be obtained easily by mechanical exfoliation using adhesive tape. Chemical method has the advantage to obtain large quantities of graphene starting from graphite. Graphene oxide is the intermediary compound (Figure 2, b) where functional groups remove and exfoliate graphene layers. Chemical reduction of GO allows to obtain a graphene form, named reduced-GO (r-GO). As a precursor of r-GO, GO is obtained by means of Hummers method *via* oxidation of graphite with a mixture of concentrated $H_2SO_4$and $KMnO_4$. GO contains various functional groups, epoxy, OH and COOH.

Unfortunately, both r-GO and GO have a lower electrical conductivity by some orders of magnitude than graphene due to an incomplete reduction and the presence of numerous structural defects that interrupt sp^2 hybridisation and conjugation in plane (2D). Graphene is a hydrophobic material and is not soluble in any organic solvent and we have used for its synthesis the known method for synthesis of GO and then its reducing to r-GO. (Figure 2 c).

Synthesis of graphene oxide (GO) by modified Hummer [10] method.

In a 500 ml three-neck flask were introduced 5 g of graphite flakes and 3.75 g sodium nitrate followed by addition of 375 ml conc. H_2SO_4. To the stirred and cooled in ice / water solution was added 22.5 g of $KMnO_4$ in an one hour. Cooling was removed after 2 hours and the reaction mixture was stirred at room temperature for 5 days. Then the reaction mixture was added to an aqueous solution of H_2SO_4 (700 mL, 5%) with stirring and the resulting mixture was heated to 98 ° C and stirred for 2 hours. Then the temperature was lowered to 60 ° C and hydrogen peroxide (15 ml, 30%) was added to reduce Mn^{7+} ions and MnO_2 to colorless $MnSO_4$. After treatment with H_2O_2 the suspension turns on as yellow colored. The precipitate was filtrate when it is still hot to remove soluble heavy metal salts. The precipitate was washed three times with a total of 14 l of hot distilled water and then dispersed again in water, centrifuged and dried in the oven.

Reducing GO

To a suspension of GO maintained at 2-5 ° C a solution of 5 mmol hydrazine was added dropwise for one hour. Graphene (R-GO) suspension was filtrate ad then washed with distilled water and dried at 70 ° C.

Characterization of GO and r-GO

FTIR spectra of graphite, GO and r-GO are shown in Figures 3-5 and show the presence of functional groups in GO and r-GO. The spectrum shows an continuous absorption for graphite in IR spectrum with two absorption peaks (1632 and 1578 cm^{-1}) assigned to C = C double bond vibration and an absorption peak at 3426 cm^{-1} assigned to absorbed water and some groups resulted from in-time oxidation of graphite. In FTIR spectrum of GO the absorption at 1735 cm^{-1} is assigned to stretching vibrations of -C = O and –COOH groups. The absorptions peaks associated with carboxyl (CO), epoxy (OCO) and alcoxi (CO) can be found at 1401, 1220 and 1069 cm^{-1}, respectively. The IR spectrum of r-GO shows fewer bands than GO and remembering IR spectrum of graphite. However, the reduction is not complete, at least carboxyl groups on the edges of the GO remain unchanged.

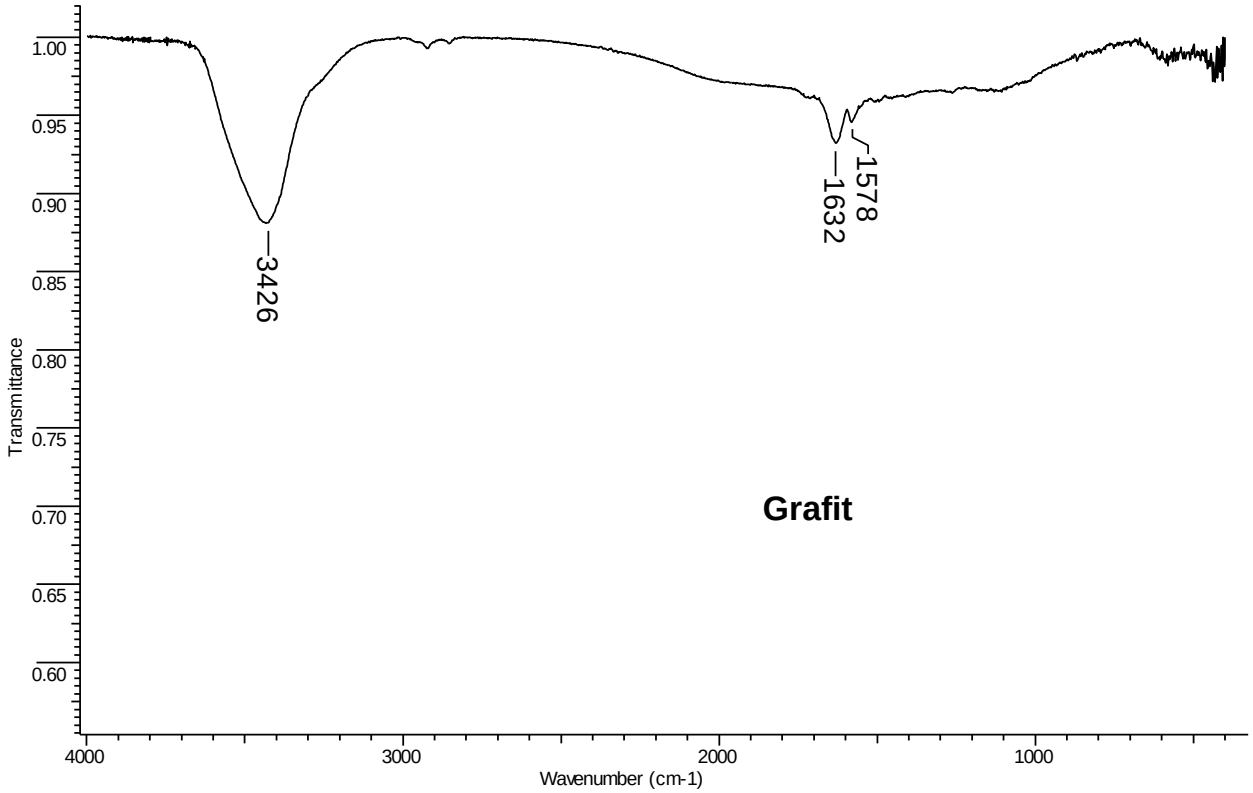

Figure 3. FTIR spectrum of graphite

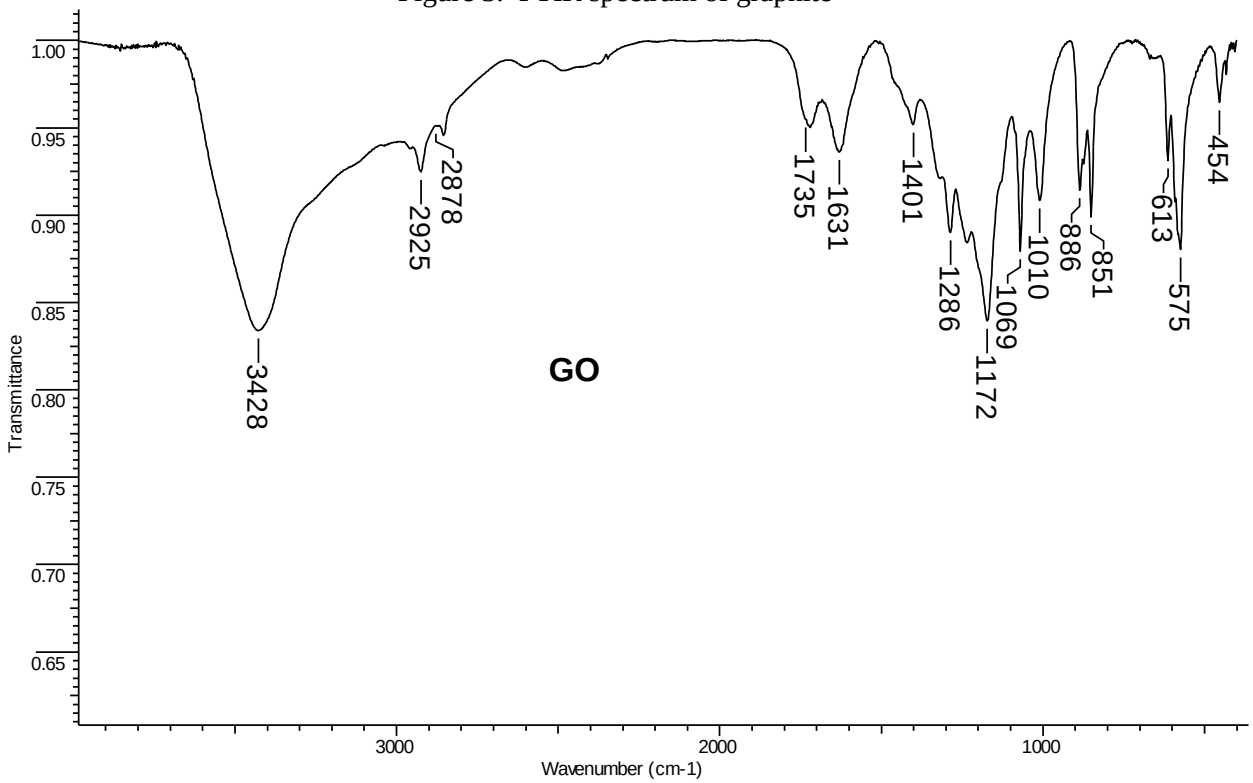

Figure 4. FTIR spectrum of graphene oxide

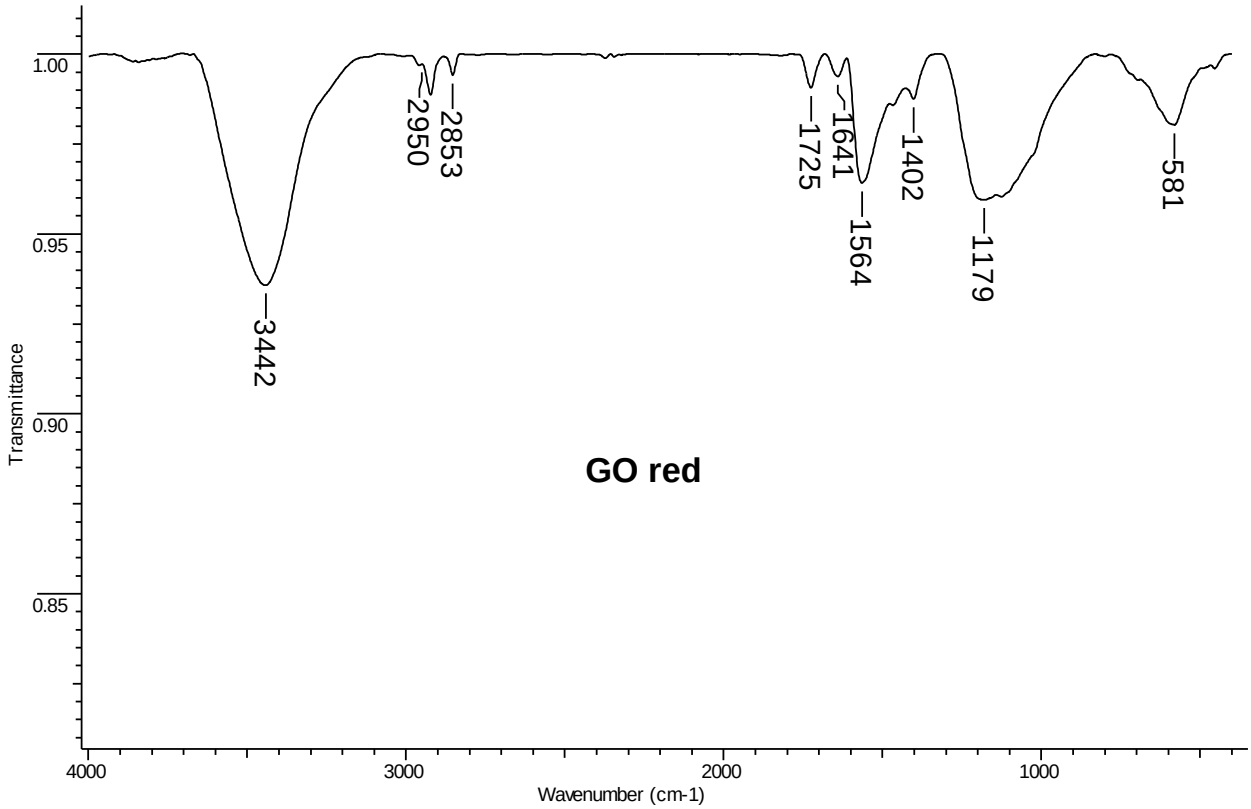

Figure 5. FTIR spectrum of graphene obtained from reduced graphene oxide

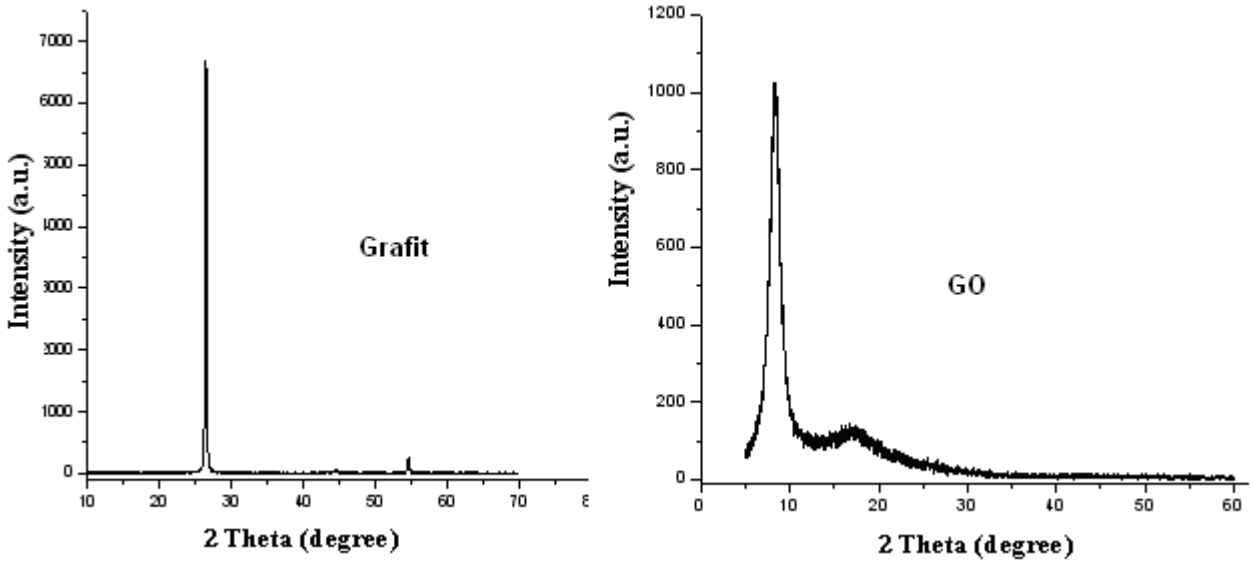

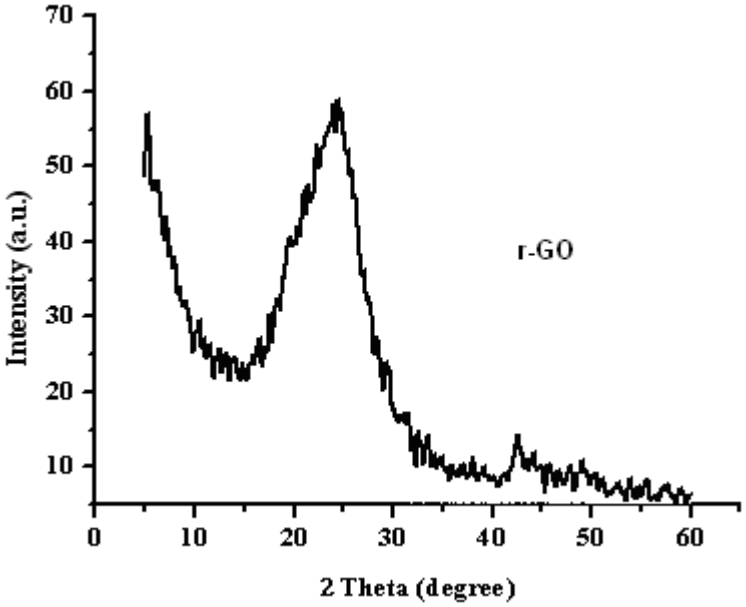

Figure 6. X-ray spectra pf graphite, grapheme oxide (GO) and graphene (r-GO).

GO shows a lamellar morphology where OH and epoxide functional groups destroy planar ad hexagonal structure of carbon and decrease van der Waals forces between layers and thus increasing distance between layers . Due to the functional groups GO can be dispersed in hydrophilic solvents. In the graphite, the distance between layers is ~ 0.33 nm and is increased to 0.79 nm in GO. This is clearly evidenced by X-ray spectra, where the maximum observed at $2\theta = 26.7^{o}$ in graphite is shifted at a $2\theta = 10.3^{o}$ characteristic for GO. Also a wider maximum of low intensity appears at $2\theta = 17.0^{o}$ indicating a less homogeneous structure of GO. After reducing of GO to the r-GO, the peak from $2\theta = 10.3^{o}$ disappears and another peak appears, much wider than in the graphite at $2\theta = 24.5^{o}$ suggesting a less ordered structure. By reducing, the OH and epoxy groups situated in basal plane disappear but edges COOH groups, remain and contribute to a greater distance between layers of 0,33 nm.

Because GO has hydrophilic functional groups it can form through ultrasonication stable aqueous dispersions. Instead, the overwhelming majority of polymer solar cells are hydrophobic and insoluble in aqueous solvents. Thus, the obtention of homogenous composites from conjugated polymers and GO in hydrophobic organic solvent is difficult. Also, r-GO due to removal by reduction of epoxy and OH groups is less hydrophobic, its water dispersions are less stable than those with GO. All our attempts to get the homogeneous films by blending of r-GO with conjugated polymers in organic solvents have failed. In order to homogeneously disperse the r-GO in the organic polymer a way would be grafting of organic compounds on graphene surface. For instance, the hydroxyl function of the GO were reacted with isocyanate and then reduced. The product is dispersible in organic solvents and can be easily mixed with conjugated organic polymers [11]. The grafting of organic compounds on graphene surface will be in our attention in the future studies.

An organic compound that can be associated with a fragment of graphene structure, and which is soluble in organic solvents is perylenediimide and its derivatives, and which is a potential compound that can replace fullerene acceptor [12].

Perylenediimides: synthesis and chracterization

3,4,9,10-Tetracarboxylic perylenediimides (Scheme 1) were discovered in 1913 by Kardos [13] and have been used as dyes for textiles first and later as a high-performance pigments [14].

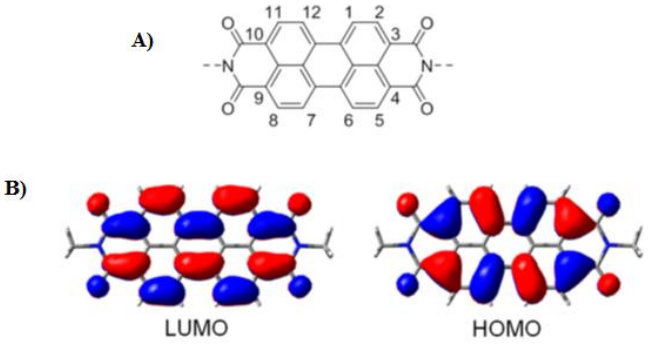

Scheme 1. A) Chemical structure of perylenediimide and, B) molecular orbitals HOMO si LUMO of perylenediimide [15]

Perylenediimides represent a class of thermostable materials with high molar absorption coefficient and a high capacity to accept electrons and with excellent transport properties [16]. Unfortunately, perylenediimides suffer from low solubility and aggregation tendency in various solvents and a low fluorescence quantum yield in solid state.
Perylenediimide structure can be modified by functionalization with alkyl or aryl groups at the nitrogen atoms or in the bay positions 1, 6, 7 and 12, and the ortho positions 2.5, 8 and 11, and this has as result an material with a better processability and good solubility in various solvents and tunned HOMO and LUMO levels [17, 18].

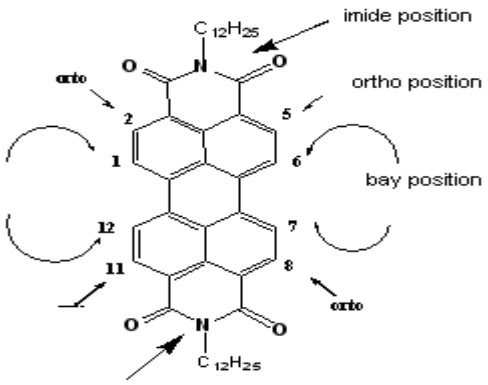

Scheme 2. The structure of perylenediimide and its reactive positions

Perylenediimide is among the first and most commonly accepted compound that can replace fullerene derivatives in heterojunction solar cells [19]. The energy efficiency of the best perylendiimide compound used in BHJ cells is 3.17% while the energy efficiency of fullerenes is 8.3%. It seems that the strong aggregation of perylenediimides is the main reason for the poor efficiency. Therefore, the controll of the acceptor/donor morphology films is a very important subject for research [18].
In the first stage we synthesized N, N-bis (dodecyl) - 3, 4, 9, 10-tetracarboxylic perylenediimide starting from 3,4.9,10-tetracarboxylic-perylendianhydride and dodecylamine in NMP and acetic acid at 85 ° C (Scheme 3)

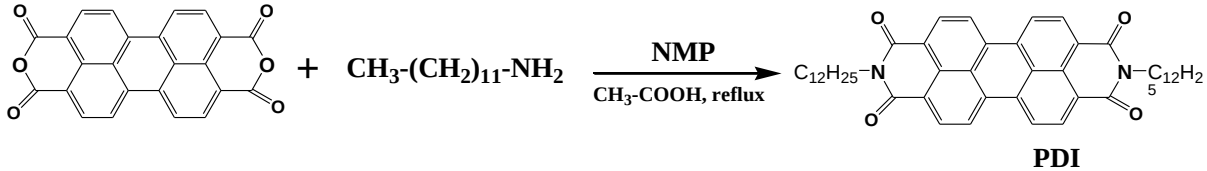

PDI

Scheme 3. Synthesis of N, N-bis(dodecyl)- 3, 4, 9, 10-tetracarboxyl perylenediimide (PDI)

The structure of the PDI was proved by spectral methods (Table 1)

Table 1: Spectral characterization of PDI si PDI-Br

Compound	***^{1}H-RMN (δ, ppm)***	***FTIR (cm^{-1}) (pastila KBr)***

PDI	8.66 (d, 4H perilena); 8.60 (d, 4H perilena); 4.20 (t, 4H, N-CH_2-); 1.77-1.80 (m, 4H, -CH_2-); 1.25-1.47 (m, -CH_2-); 0.88-0.91 (m, 6H, -CH_3).	3430, 3063, 2954, 2923, 2849, 1696, 1656, 1592, 1508, 1463, 1438, 1374, 1345, 1252, 1088, 1019, 850, 809, 746, 726, 629, 436.
PDI-Br	9.45 (d, 2H), 8.89 (s, 2H), 8.70 (d, 2H), 4.19 (t, 4H, N-CH_2), 1.74 (m, 4H, -CH_2-), 1.25-1.43 (m, 36H, -$(CH_2)_9$-), 0.85-0.89 (m, 6H, -CH_3).	3430, 3063, 2954, 2920, 2848, 1700, 1662, 1593, 1506, 1463, 1434, 1394, 1339, 1239, 1158, 1090, 858, 810, 747, 723, 683, 537

UV-Vis and fluorescence spectra of the PDI compounds were registered in chloroform solution. Optical data are summed in Table 2 and illustrated in Figure 7. UV-Vis spectrum shows absorption bands typical for π-π * electronic transitions of the perylenediimide chromophore. Emission spectrum shows a vibronic structure and appears as the mirror image of the absorption spectrum.

Table 2. Optical data of PDI si PDI-Br in chloroform solution

Compuound	λ_{abs}^{max} (nm)	λ_{em}^{max} (nm)
PDI	462, 490, 528	536, 575, 621 (ex. 490, 528)
PDI-Br	462, 489, 528	550, 585 (sh) (ex.489, 528)

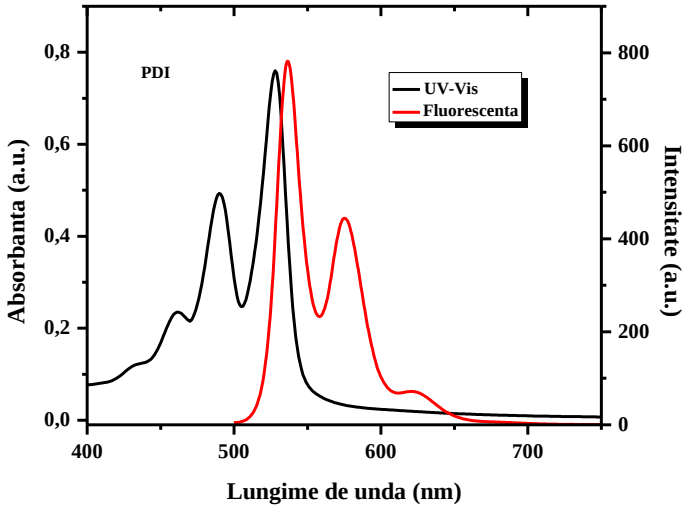

Figure 7. Absorption and emission spectra of PDI in $CHCl_3$ solution.

Electrochemical properties, HOMO and LUMO energy levels of the PDI compound are shown in Table 2 and cyclic voltammetry curve is shown in Figure 8. The redox properties of this compound have shown that HOMO and LUMO energy levels have values close of the fullerenes and recommend this acceptor material to replace fullerene derivatives.

Table 3: Electrochemical data of **PDI**

Compound	E_{ox}^{onset} (V)	E_{red}^{onset} (V)	E_{HOMO} (eV)	E_{LUMO} [a] (eV)	E_g^{op} [b] (eV)
PDI	---	-0.93	-5.70	-3.44	2.26

[a] $E_{LUMO} = -e(E_{red}^{onset} + 4.37)$ (eV)

[b] $E_g = E_{LUMO} - E_{HOMO}$

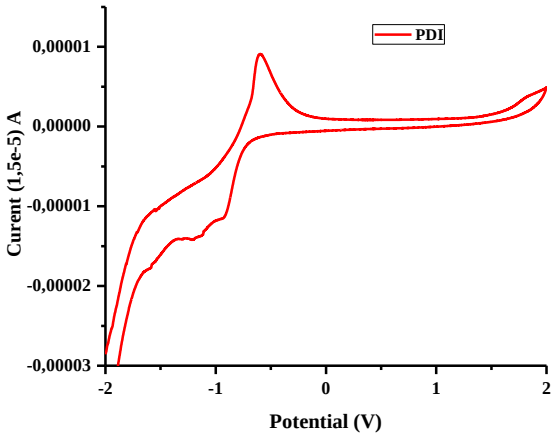

Figure 8. Cyclic voltammetry of PDI, in acetonitriel and tetrabutylamonium perchlorate as electrolyte (TBAP) (10^{-1} M).

In the next step PDI was functionalized with bromine atoms, i.e., 1,7-dibrom- N, N-bis-dodecyl- 3, 4, 9, 10-tetracarboxyl perylenediimide (PDI-Br), to be used for covalent linking in copolymer structures.

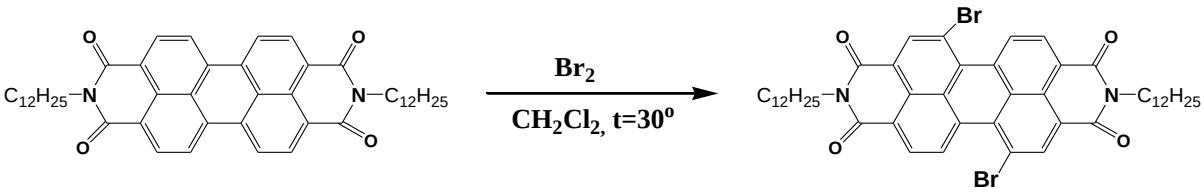

PDI **PDI-Br**

Scheme 4. Synthesis of 1,7-dibrom- N, N-bis(dodecyl)- 3, 4, 9, 10-tetracarboxyl perylenediimide (PDI-Br)

FTIR and NMR spectra prove the chemical structure of PDI-B (Table 1).
UV-Vis and fluorescence spectra of the PDI-Br were recorded in chloroform solution (Figure 9). and relevant optical data are summed in Table 2. If we analyze the absorption spectra of the two compounds (PDI and PDI-Br) is can be seen there are minor differences between them. In the fluorescence spectra of PDI-Br, the emission band from 621 nm disappears, and the other two shifted to higher wavelengths than those of the PDI compound appear.

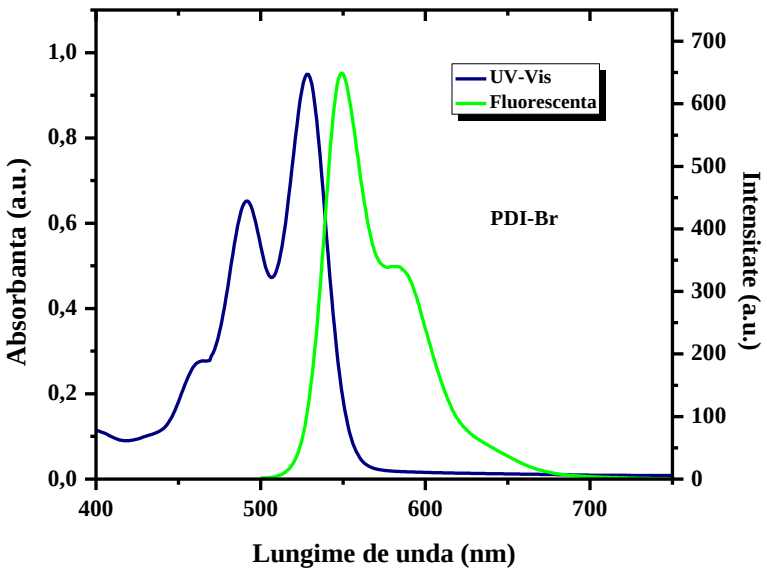

Figure 9. Absorption and emission spectra of PDI-Br in $CHCl_3$

Polymer/perylenedimide films: morphology and UV/photoluminescence studies

The first acceptor compound, PDI, has been used to obtain blends with carbazole-based polymers (their synthesis has been reported in previous years , 2013), i.e., poly (N- (2-ethylhexyl) 2,7-carbazolyl-vinylene (P1) and poly (N- (2-ethylhexyl) 3, 6-carbazolyl -vinylene (P3) (Scheme 5). Mixtures of polymer / PDI were dissolved in chloroform and deposited on transparent ITO electrode for spectroscopic and morphological studies and in perspective for use as active layer in solar cells.

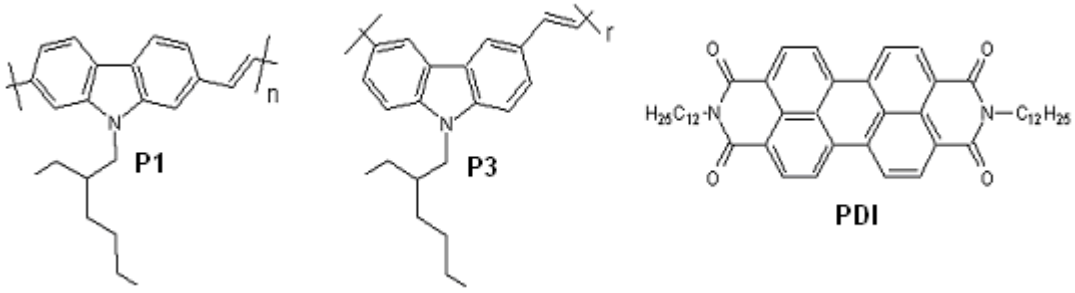

Scheme 5. Chemical structure of donor polymers and acceptor used as photovoltaic films

Solutions for spin-coating were made as follows:

a) 0.06 g of P3 + 18ml chloroform, resulting in a solution concentration of $0.101x10^{-1}$ mol / L

b) 0.06 g of P1 + 18 ml chloroform, resulting a solution of $0.101x10^{-1}$ mol / L concentration.

c) 0.02 g of PDI + 6 ml chloroform, resulting a solution of $0.46x10^{-2}$ mol / L concentration.

d) 0.04 g of PDI + 6 ml chloroform, resulting a solution of $0.91x10^{-2}$ mol / L concentration.

e) 0.06 g of PDI + 6 ml chloroform, resulting a solution of $1,375x10^{-2}$ mol / L concentration.

The final solutions used for spin coating were made, without further ultrasonication, as follows:

1. 2ml of P3 in chloroform(from solution a)) mixed with 2 ml of PDI in chloroform (solution c) ;- P3/PDI ratio = 1:1.
2. 2ml P3 solution with 2 ml of PDI (solution d) ; P3/PDI ratio = 1:2.
3. 2ml P3 solution with 2 ml of PDI (solution e); P3/PDI ratio = 1:3.
4. 2ml P1 (solution b) with 2 ml of PDI (solution c); P1/PDI ratio = 1:1.
5. 2ml P1 solution with 2 ml of PDI (solution d); P1/PDI ratio = 1:2.
6. 2ml P1 solution with 2 ml of PDI (solutia e); P1/PDI ratio = 1:3.

ITO substrates of 33-45 Ω, were cutted to electrodes with 2.5*1.5 cm dimensions and were washed in ultrasonic bath at 50^0C with:

- Hot water and detergent for 25 minutes;
- Acetone, 45 minutes;
- Izopropanol, 25 minutes;
- Drying in nitrogen atmosphere.

The films were made using fresh-prepared solutions after the substrates were treated in oxygen plasma at full power for 10 minutes, by "spin coating" in a clean room, in less than 20 minutes after plasma treatment.

Morphology of polymer and polymer/acceptor films prepared by spin coating

P3 on ITO (5μmx5 μm)

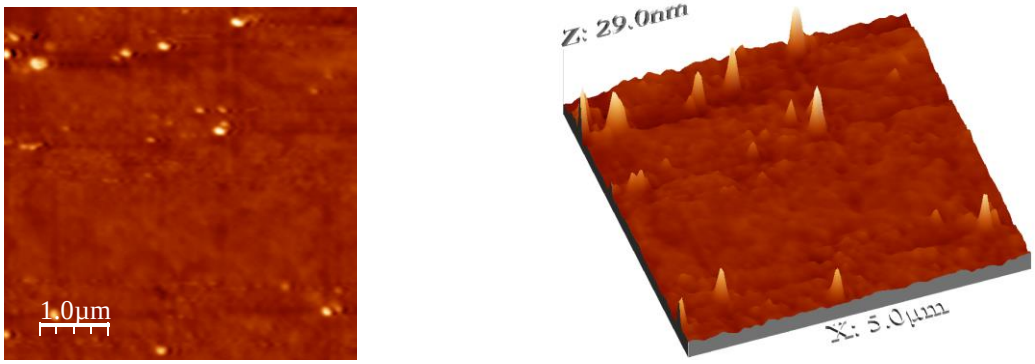

RMS=1,37 nm; RA=0,74 nm

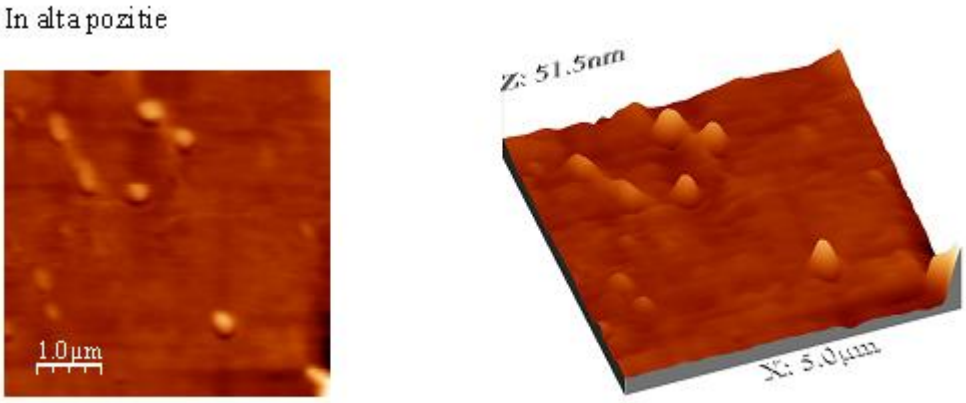

RMS=2,7 nm; RA=1,6 nm

Figure 10. Morphology of P3 films

Conclusion: regardless of layer position, the roughness of resulting film is small.

PDI on ITO (5µmx5 µm)

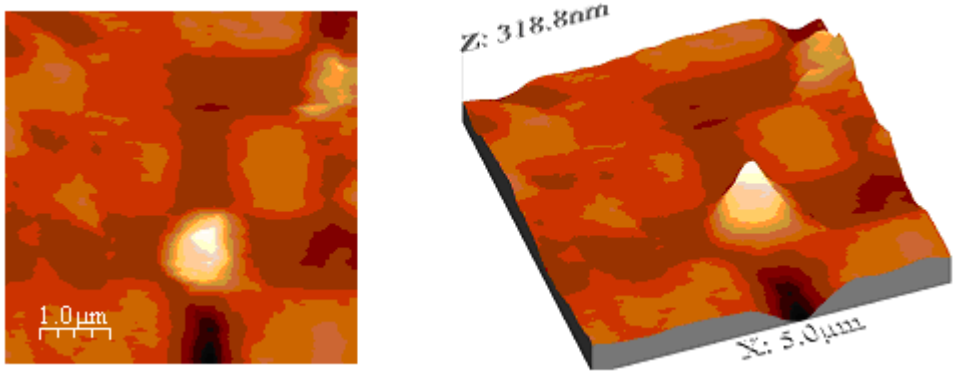

RMS=32,3 nm; RA=21,9 nm

In alte zone.

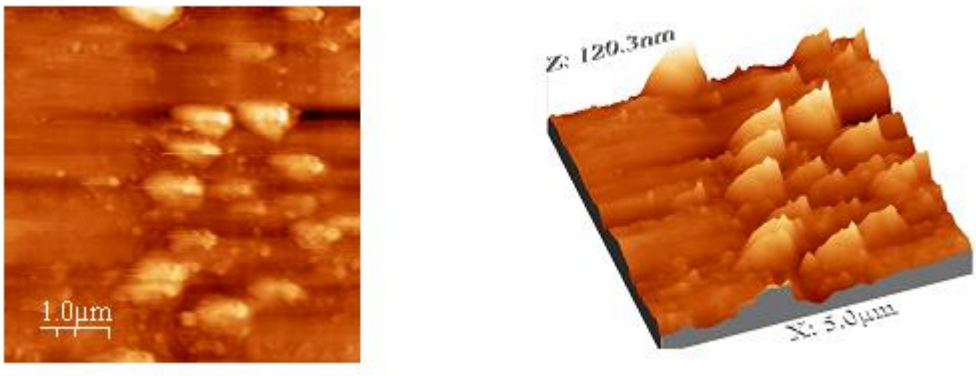

RMS=12,6 nm; RA=8,7 nm

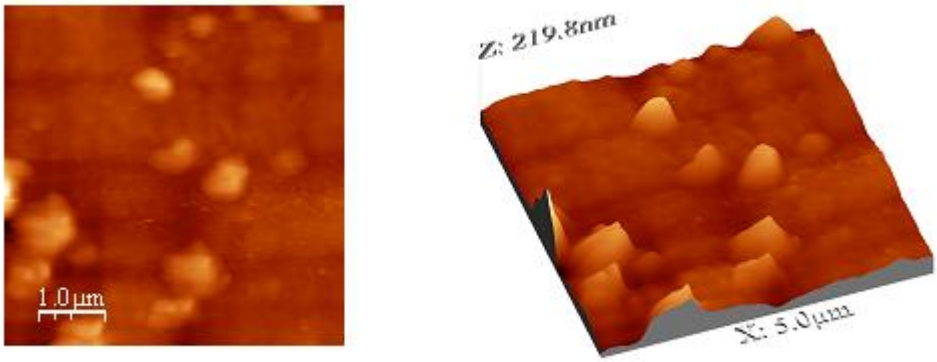

RMS=16,7 nm; RA=11 nm

Figure 11. Morphology of acceptor (PDI) film.

P1/PDI (5µmx5 µm)

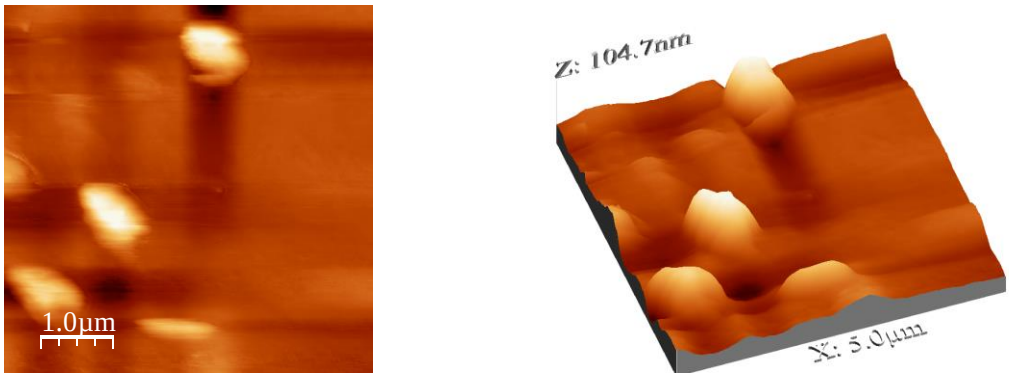

RMS=11,9 nm; RA=7,5 nm

In alte pozitii pe strat

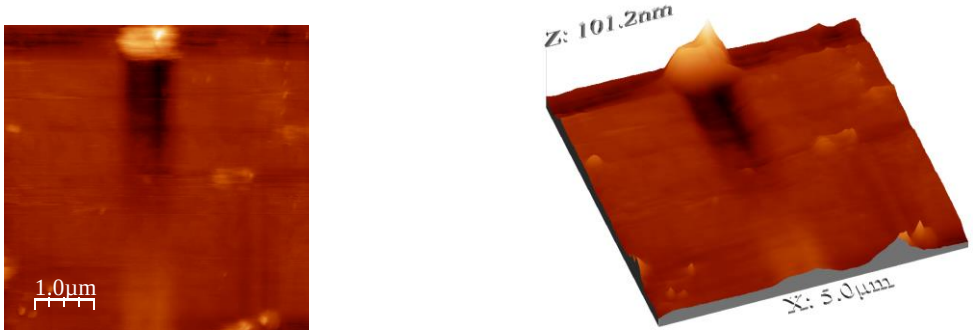

RMS=6.70 nm; RA=3,98 nm

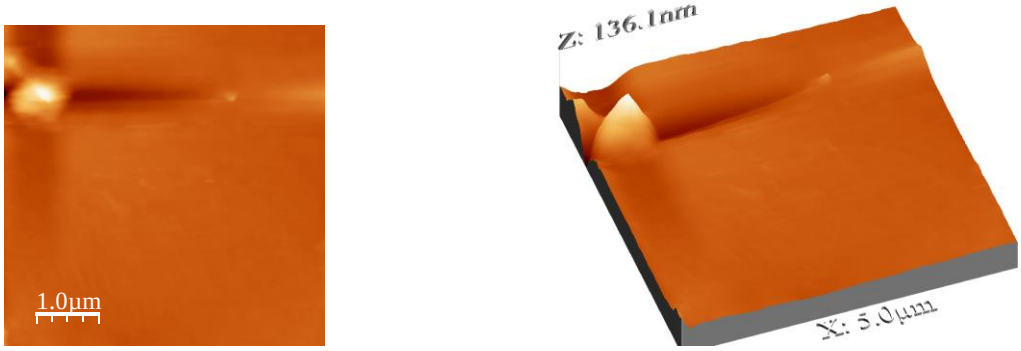

RMS=7,02 nm; RA=3,69 nm

Figure 11. Morphology of donor/acceptor, P1/PDI, film

Conclusions: For P1/PDI layer, the roughness is higher than for individual partners. A greater roughness is associated in principle with a worse contact with the Al electrode and therefore a smaller number of charge carriers are collected.

P3/PDI (5µmx5 µm)

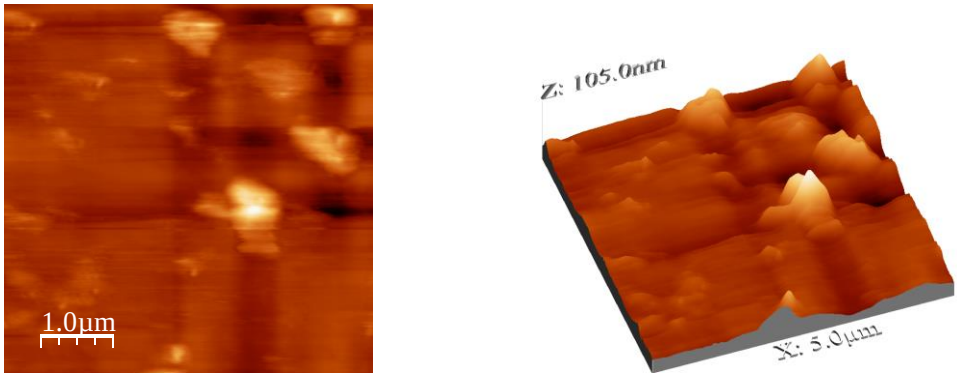

RMS=8,9 nm; RA=5,5 nm.

Other surfaces:

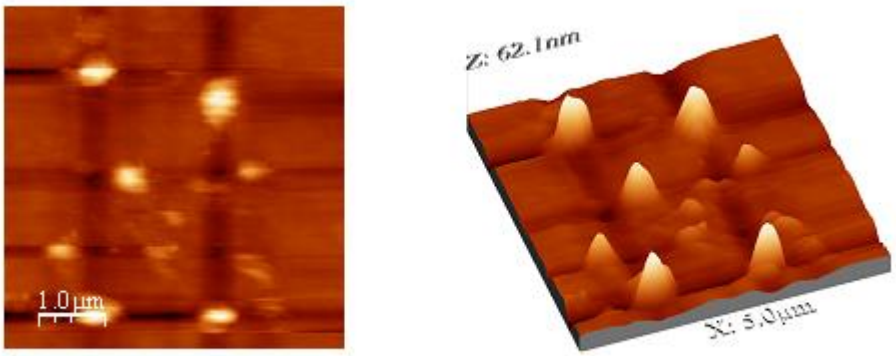

RMS=5,7 nm; RA=3,4 nm

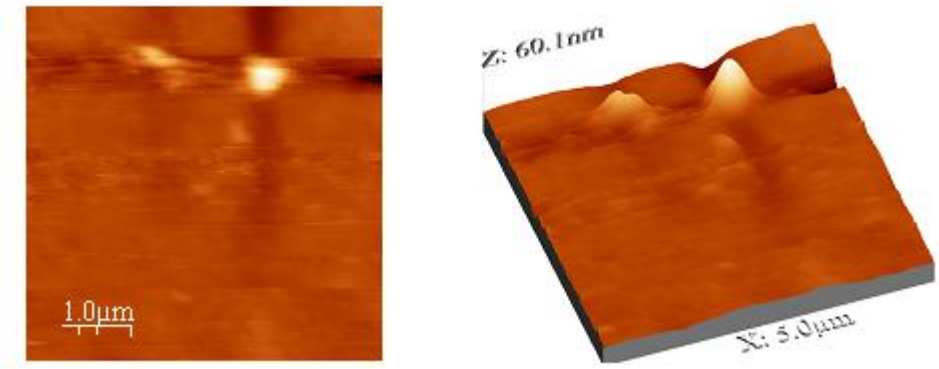

RMS=3,5 nm; RA=1,8 nm.

Figure 12. Morphology of donor polymer/acceptor, P3/PDI, films.

Conclusion: It is observed that the films obtained by spin-coating are non-uniform deposited, the roughness varies from one area to another for the same layer. PDI film has roughness compared to P3. By mixing it with P3 the layer roughness is much smaller, even than the mixed layer P1 / PDI.

UV-Vis measurements of P1, P3 and PDI samples prepared by spin-coating on ITO support.

1. The effect of donor polymer type: P3 and P1.
In the polymer/PDI mixture, the dominant effect is assigned to the polymer P3 or P1, the shape of absorption edge is determined mainly by P3 and P1.
2. The effect of the acceptor concentration, P3 / P1: PDI= 1: 1; 1: 2 and 1: 3.
Increased levels of PDI did not lead to significant changes in the shape of the edge absorption

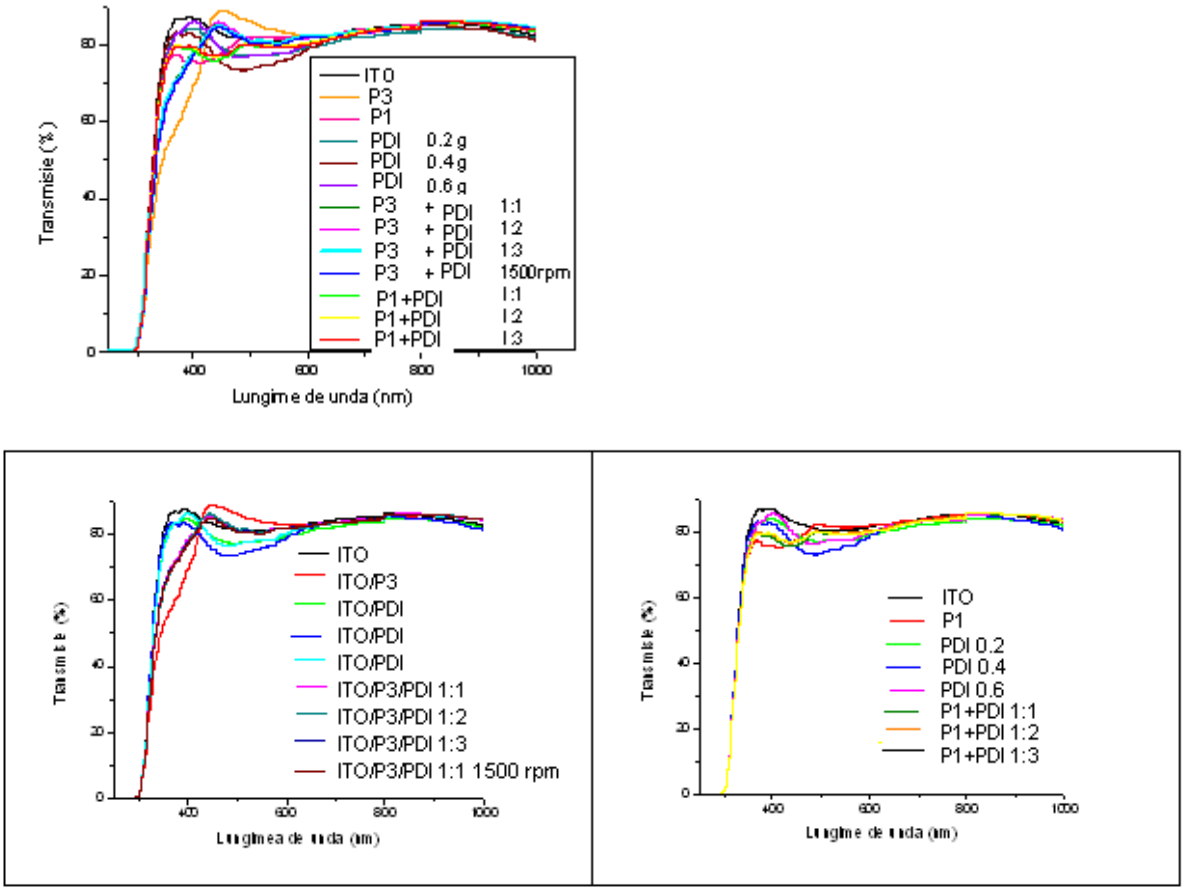

Figure 13. UV-Vis spectra of P3, P1, PDI and their mixtures: P3:PDI si P1:PDI

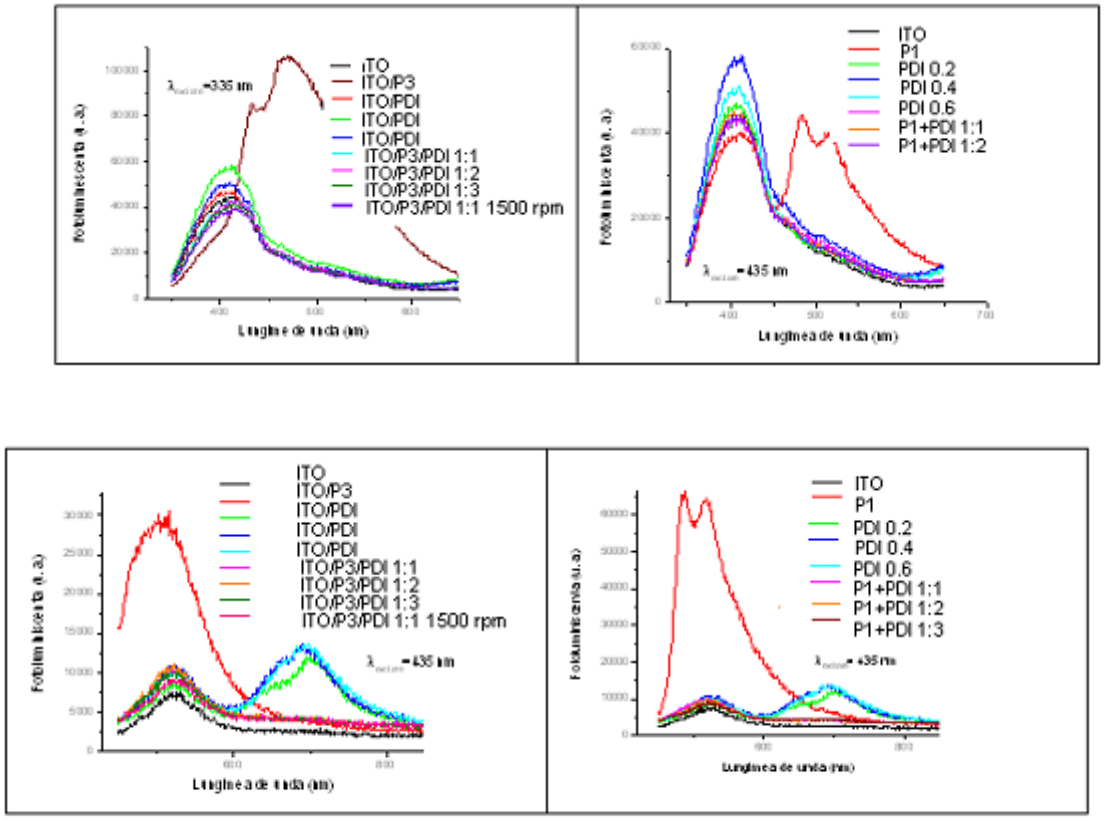

Figure 14. Photoluminescence spectra of polymer films P3, P1, PDI and mixed P3/PDI and P1/PDI in 1:1, 1 :2 si 1:3 ratio for pentru $\lambda_{excitare}$=335 nm and 435 nm

For $\lambda_{excitare}$ = 435 nm, the polymer P3 has an intense photoluminescence centered at 520 nm, the polymer P1 had a strong emission splitted, with two peaks located ~ 490 nm and 530 nm, and the acceptor PDI has two weak emission bands centered on 520 nm and 700 nm with a shoulder around 670 nm. In the mixed layer, the peak emission at higher wavelengths disappears while that of 520 nm is more attenuated. In conclusion, for mixed layers the loss of excitons by photoluminescence is reduced.

For $\lambda_{excitare}$ = 335 nm, the polymer P3 has an intense photoluminescence emission, with two peaks centered on 450 nm and 500 nm. In the mixed layer, the emission disappears and appears a much weaker band centered on 430 nm assigned to PDI compound. The intensity of the emission band does not vary significantly with increasing content of PDI. For the polymer P1, there are 2 emission bands, one with a maximum at 430 nm and one split with two peaks located at 490 nm and 530 nm. The second emission band disappears by adding PDI, the increase of PDI concentration has not a significantly effect.
It can say that by adding of PDI acceptor to P3 and P1 polymeric material the photoluminescence intensity decreases due to door/acceptor complex formation.

Observation: Photovoltaic properties of the polymeric films will be studied in the 2016

Donor /acceptor copolymers with carbazole and perylenediimide groups

In parallel, the PDI group was covalently introduced in the polymer chains P1 and P3, through a copolymerization reaction. Thus, two poly(arylenevinylene) copolymers containing 3,6- or 2,7- disubstituted carbazole and perylenediimide groups were synthetized through Stille coupling reaction using as vinylation agent, 1,2-bis(tributylstannyl)ethane.

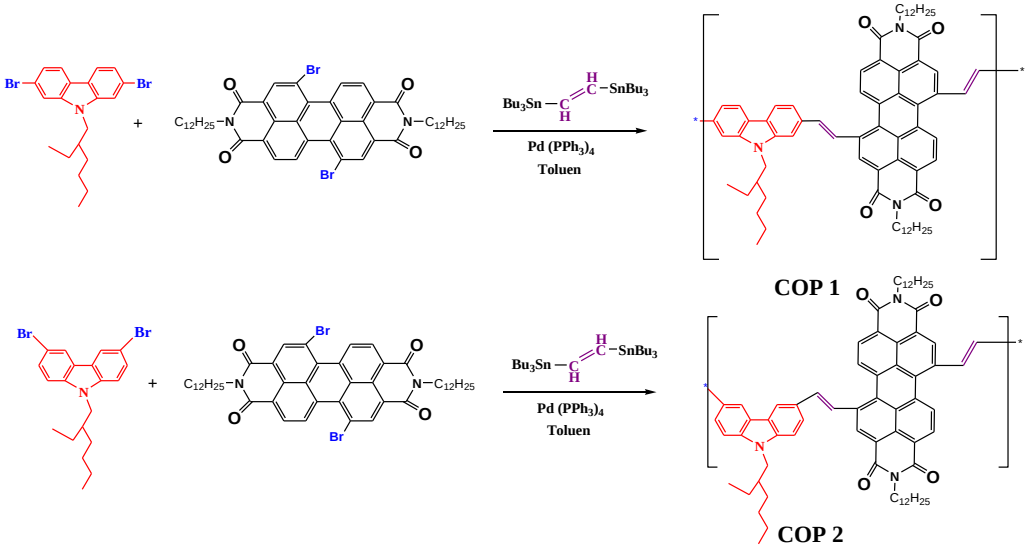

Scheme 6: Synthesis of poly(arylene-vinylene)s copolymer

Molecular structures of copolymers were confirmed by FTIR and ^{1}H-NMR analyses.

The thermal properties of the resulting copolymers were measured by TGA under nitrogen atmosphere (Figure 15). The high onset decomposition temperatures (T_d) (~5% weight loss) in the range 420-440^{o}C for these compounds suggest that they exhibit very good thermal stability. We employed differential scanning calorimetry to investigate any phase transitions, but no transitions were observed.

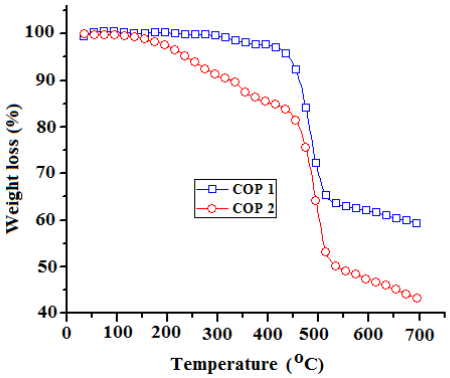

Figure 15. TGA thermogram of the copolymers

The cyclic voltammetric behavior of copolymers was studied in acetonitrile solution containing 0.1 M TBAP as supporting electrolyte with a scan rate of 50 mV s^{-1}. A platinum disc electrode was coated with thin film and was used as the working electrode. The cyclic voltammograms of polymer films (COP1 -COP2) versus Ag/Ag^{+} are illustrated in Figure 16 and cyclic voltametry results of copolymers are summarized in Table 4. Electrochemical oxidation of copolymers starts at about 1.17 V (COP 1) and 1.12 V (COP 2) vs. Ag/Ag^{+}, respectively. As can be seen from Figure 16, the electrochemical oxidation assigned to the oxidation of carbazole unit is irreversible. This irreversibility attributed to carbazole, is also observed in some carbazole-like polymers with donor-acceptor groups [21]. The onset reduction potential is estimated at -0.92 V for COP 1 and -0.95 V for COP 2. From the onset value of oxidation potential and reduction potential, the highest occupied molecular orbital (HOMO) energy level and lowest occupied molecular orbital (LUMO) as well as the electrochemical band gaps (E_g^{el}) of the copolymers were determined using ferrocene/ferrocenium (Fc/Fc^{+}) as an internal standard (the ionization potential of the Fc/Fc^{+} is -4.8 eV) and its redox potential measured by us is 0.43V versus Ag/AgCl. The energy levels of polymers can be obtained using the equations: $E_{HOMO} = -e\ (E_{ox}^{onset} - E_{ferrocene}^{1/2} + 4.8)$ (eV) and $E_{LUMO} = -e\ (E_{red}^{onset} - E_{ferrocene}^{1/2} + 4.8]$ (eV). The HOMO and LUMO energy levels of the films copolymers are -5.54 eV (COP 1), -5.49 eV (COP 2) and. -3.45 eV (COP 1),-3.42 eV (COP 2), respectively.

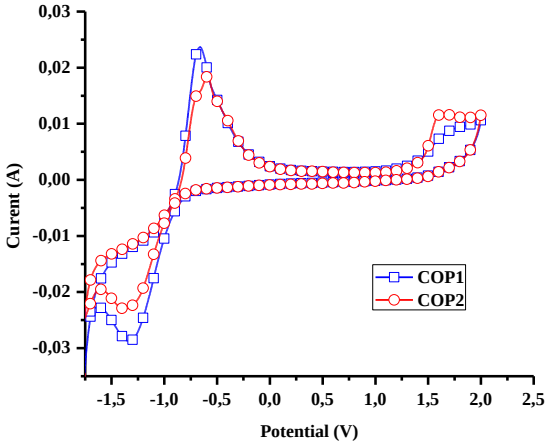

Figure 16. Cyclic voltamograms of copolymers

Table 4. Electrochemical properties of the copolymers

Sample	E_{ox}^{onset} (V) vs Ag/AgCl	E_{red}^{onset} (V) vs Ag/AgCl	E_{HOMO} [a)] (eV)	E_{LUMO} [b)] (eV)	E_g^{el} [c)] (eV)
COP1	1.17	-0.92	-5.54	-3.45	2.09
COP2	1.12	-0.95	-5.49	-3.42	2.07

a $E_{HOMO} = -e(E_{ox}^{onset} + 4.37)$ (eV).

[b] E_{LUMO} = -e(E_{red}^{onset} +4.37) (eV), where E_{ox}^{onset} and E_{red}^{onset} are the onset of oxidation and reduction potential, respectively of the copolymers versus Fe/Fe^{+}.
[c] Electrochemical band gap calculated from HOMO and LUMO energy levels.

The UV-Vis absorption spectra of two copolymers in chloroform solution and thin film are show in Figure 17 and the corresponding data are summarized in Table 5. The absorption spectrum of copolymer solution displayed two distinct maxima at 435 and 586 nm for COP 1 and three distinct peaks for COP 2 at 314, 346 and 576 nm for. The absorptions bands at the shorter wavelengths (346- 435 nm) are owed to the π-π^{*} transitions of the carbazole unit, while the bands at wavelengths higher are assigned to perylenedimide groups (585 and 576 nm). The absorption maxima of copolymers specific to perylenediimide were red-shifted by 58 nm for COP 1 and 48 nm for COP 2 compared with that of pure PDI-Br. By making a comparison between the UV-Vis spectra of solution of copolymers and thin film it can be observed that the absorption spectra are very similar with notification that the spectra measured in solution were red-shifted in contrast with their films, as seen in Table 5.

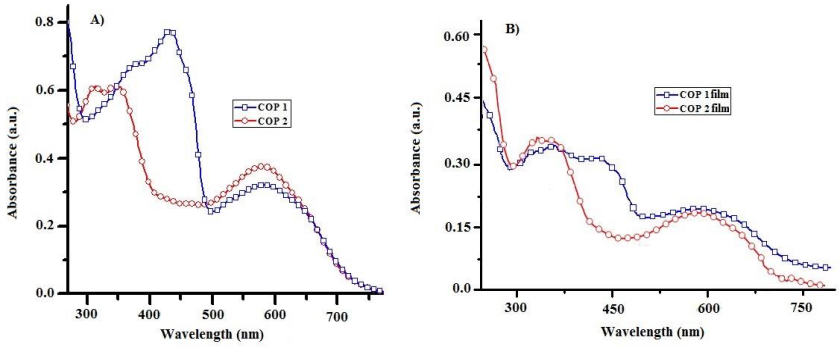

Figure 17. Absorption spectra ($CHCl_3$) of copolymers A) solution, B) film

Table 5. Optical data of copolymers

Sample	Solution		Film	E_g^{op}
	λ^{abs}_{max} (nm)	λ^{em}_{max} (nm)	λ^{abs}_{max} (nm)	(eV)
PDI-Br	462, 489, 528	550 (ex.489) 585 (ex. 528)	-----	-----
COP1	435, 586	462 (ex. 435) 676 (ex.586)	435, 585	1.60
COP 2	314, 346, 576	425 (ex. 346) 680 (ex.576)	336, 580	1.65

The fluorescence spectra of copolymer in chloroform solution are shown in Figure 18 and corresponding data are summarized in Table 5. The PL emission spectra were recorded at 435 and 586 nm excitation for COP 1 and by excitation at 346 and 576 nm for COP 2. It seems that the emission spectrum of copolymer excited with the wavelength specific to perylenediimide were red-shifted compared to PDI-Br (peaks values of fluorescence spectra of this monomer are illustrated in Table 5. The PL spectra of copolymer COP 1 excited with the wavelength specific to carbazole units (435 nm) is bathochromic shifted with 37 nm compared to fluorescence spectra of COP 2 excited with 346 nm. This is due to the fact that carbazole units substituted at 2,7-positions show a longer conjugation path through biphenylene units from the carbazole and the spacer, while for copolymer having 3,6-substituted carbazole units, the conjugation takes place between phenyl units and spacer through lone electron pair of carbazole nitrogen.

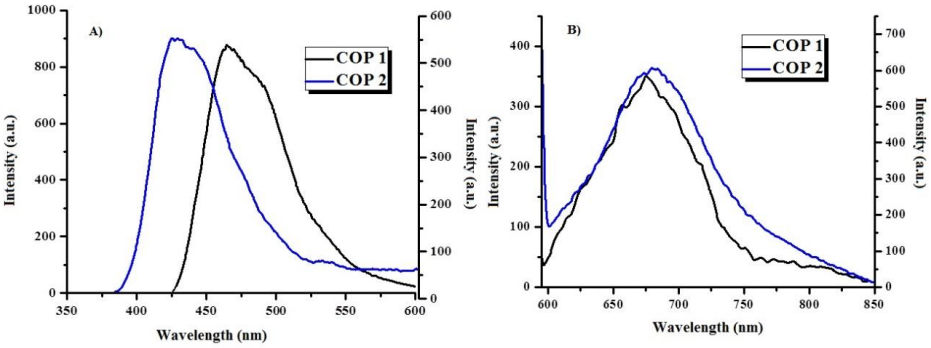

Figure 18. Emission spectra ($CHCl_3$-solution) of copolymers A) excited with the wavelength specific to perylenediimide, B) excited with the wavelength specific to carbazole units

The energy levels values (HOMO and LUMO) were calculated from the cyclic voltammetry. These results indicate that compounds can be used in bulk heterojonction solar cells where the perylenediimide as acceptor and carbazole units as donor.

References

[1] Y. Huang,E. J. Kramer, A. J. Heeger, G. C. Bazan, *Bulk Heterojunction Solar Cells: Morphology and Performance Relationships*, Chem. Rev., 114 (14), pp 7006–7043 (2014).

[2] Y.J. Cheng, S.H. Yang, C.S. Hsu, *Synthesis of Conjugated Polymers for Organic Solar Cell Applications*, Chem. Rev., 109 (11), pp 5868–5923 (2009)

[3] Y. Li, *Molecular Design of Photovoltaic Materials for Polymer Solar Cells: Toward Suitable Electronic Energy Levels and Broad Absorption*, Acc. Chem. Res., 2012, 45 (5), pp 723–733

[4] J. Roncali, *Molecular Bulk Heterojunctions: An Emerging Approach to Organic Solar Cells*, Acc. Chem. Res., 42, 1819-1830 (2009)

[5] A.K. Geim and K.S. Novoselov, *The rise of graphene*, Nat. Mater. 6 (2007), pp. 183–191.

[6] A.C. Neto, F. Guinea, and N.M.R. Peres, *Drawing conclusions from graphene*, Phys.World 19 (2006), pp. 33–37.

[7] K.S. Novoselov, A.K. Geim, S.V. Morozov, D. Jiang, Y. Zhang, S.V. Dubonos, I.V. Grigorieva,
and A.A. Firsov, *Electric field effect in atomically thin carbon films*, Science 306 (2004), pp. 666–669.

[8] K.S. Novoselov, A.K. Geim, S.V. Morozov, D. Jiang, M.I. Katsnelson, I.V. Grigorieva, S.V. Dubonos, and A.A. Firsov, *Two-dimensional gas of mass-less Dirac fermions in graphene*, Nature 438 (2005), pp. 197–200.

[9] F. Rozploch , J. Patyk , J. Stankowski , Acta Phys. Pol., *A* 2007 , *112* , 557.

[10] W. S. Hummers and R. E. Offema, *Preparation of Graphite Oxide*, J.Am Chem. Soc., Vol. 80, No. 6, 1958, p.1339.

[11] [Z. Liu, Q. Liu, Y. Huang, Y. Ma, S. Yin, X. Zhang, W. Sun, Y. Chen, *Organic photovoltaic devices based on a novel acceptor material: graphene*, Adv. Mater., 20, 3924-3930, 2008].

[12] H. Imahori, T. Umeyama, S. Ito, *Large π-Aromatic Molecules as Potential Sensitizers for Highly Efficient Dye-Sensitized Solar Cells*, Acc. Chem. Res., 42, 1809-1818 (2009)

[13] Kardos M. D.R.P. 276956 Oct 10 1913. Friedlanders Fortschr Teerfarbenfabr, 1917;12, pp. 492.

[14] H.M. Smith, M. Greene, High performance pigments, Chaper 16, 2003, pp. 249-261.

[15] F. Würthner, C. R. Saha-Möller, B. Fimmel, S. Ogi, P. Leowanawat, D, Schmidt, *Perylene Bisimide Dye Assemblies as Archety pe Functional Supramolecular Materials*, Chemical Reviews, 2015, DOI: 10.1021/acs.chemrev.5b00188.

[16] G.D. Sharma, M.S. Roy, J.A. Mikroyannidis, K.R. Justin Thomas, *Synthesis and characterization of new perylene bisimide (PBI) derivative and its application as electron acceptor for bulk heterojunction*, Organic Electronics, 13, 2012, pp. 3118-3129.

[17] E.Kozma, M. Catellani, *Perylene diimide base material for organic solar cell*, Dyes and Pigmets, 98, 2013, pp 160-179.
[18] C. Li, H. Wonneberger, *Perylene Imides for Organic Photovoltaics: Yesterday, Today, Tomorrow*, Advaned Materials, 24, 2012, pp. 613-636.
[19] J. E. Anthony, *Chemistry of Materials Review,Small-Molecule, Nonfullerene Acceptor for Polymer Bulk Heterojunction*, Organic Photovoltaics, 23, 2011, 583-590.
[20] M. Murugavelu, P. K. M. Imran, K .R. Sankaran, S. Nagarajan, *Self-assembly and photophysical properties of a minuscule tailed perylene bisimide*, Materials Science in Semiconductor Processing, 16, 2013, pp. 461–466.
[21] J. Du, Q. Fang, X. Chen, S. Ren, A. Cao, B. Xu, *Synthesis and properties of poly(arylenevinylene)s comprising of an eletron-donating carbazole unit and an electron accepting 2,1,3- benzothiadiazole (or fluorene) unit in the main chain*, Polymer, 46, 2005, 11927-11933